Accurate dynamical structure factors from ab initio lattice dynamics: The case of crystalline silicon

Accurate Dynamical Structure Factors from *Ab initio* Lattice Dynamics: The Case of Crystalline Silicon.

A. Erba,[1] M. Ferrabone,[1] R. Orlando,[1] and R. Dovesi[1]

[1] *Dipartimento di Chimica IFM and Centre of Excellence NIS (Nanostructured Interfaces and Surfaces), Università di Torino, via P. Giuria 5, I-10125 Torino (Italy)*

(Dated: September 4, 2012)

A fully *ab initio* technique is discussed for the determination of dynamical X-ray structure factors of crystalline materials which is based on a standard Debye-Waller harmonic lattice dynamical approach with all-electron atom-centered basis sets, periodic boundary conditions and one-electron Hamiltonians. This technique requires an accurate description of the lattice dynamics and the electron charge distribution of the system. The main theoretical parameters involved and final accuracy of the technique are discussed with respect to the experimental determinations of the X-ray structure factors at 298 K of crystalline silicon. An overall agreement factor of 0.47 % between the *ab initio* predicted values and the experimental determinations is found. The best theoretical determination of the *anisotropic displacement parameter*, ADP, of silicon is here 60.55 $\times 10^{-4}$ Å^2, corresponding to a Debye-Waller factor $B = 0.4781$ Å^2.

I. INTRODUCTION

Nowadays, a variety of solid state *ab initio* quantum chemical methods is available for the study of many properties of the ground state of crystals at zero temperature and, for any feature to be simulated, particular prescriptions can be found in the literature which guarantee given accuracies for the computed values.[1–4] However, the experimental determination of many solid state properties such as the equilibrium structure, vibrational spectrum, electron charge and momentum density, structure factors and the directional Compton profiles is rarely obtained at very low temperature. It follows that, in order to compare the outcomes of an experiment to those of a simulation, the inclusion of temperature effects on computed quantities would be desirable.

The most performing technique for the inclusion of temperature in the computed properties of crystals would be *ab initio* molecular dynamics;[5–7] however, for the time being, it is costly and cannot be used routinely without large computational resources. The interest in developing sufficiently accurate, though approximated, models for the inclusion of temperature in standard *ab initio* quantum chemical methods, at least for some properties, follows quite naturally.

We have recently presented elsewhere[8] an *ab initio* Monte Carlo technique for the determination of the thermally averaged electronic first-order density matrix (DM) of crystals, in a harmonic approximation. All the above mentioned one-electron properties can be computed at any temperature within such a scheme in a general and homogeneous way.

In this paper we restrict our attention to *dynamical* X-ray structure factors (XSF) of crystalline materials and we present the results of accurate, fully *ab initio*, calculations within the harmonic approximation to the lattice potential. If a harmonic lattice potential is considered then the probability density functions of the nuclear displacements with respect to the equilibrium configuration of the atoms turns out to be a Gaussian function.[9] In general, the *Gaussian approximation* is not always fully justified[10,11] so that one would need an anharmonic treatment of the lattice potential which, however, is beyond the aim of this study (when there are no light atoms and temperatures close to the melting point are avoided the harmonic approximation usually provides a reliable description of the lattice dynamics of a crystal). The most common way nuclear motion effects are dealt with when X-ray diffraction is considered is by means of Debye-Waller (DW) atomic factors which damp the diffraction intensities with respect to increasing wave number and temperature. Atomic DW factors are usually computed from atomic anisotropic displacement parameters (ADP) fitted to the experiment via sophisticated spherical models that, beside temperature, are supposed to take into account a variety of aspects such as anharmonicity, atomic asphericity, thermal diffuse scattering, etc.[9,12,13] Besides, it has recently been suggested that ADPs are scarcely affected by anharmonicity so that harmonic mean-square displacements already provide a good description even of strongly anharmonic nuclear potentials.[14]

We present here a fully *ab initio* approach for the computation of ADPs, DW factors and dynamical XSFs in the frame of one-electron Hamiltonians (Hartree-Fock, HF, any kind of functional within the density functional theory, DFT, or hybrids like the popular B3LYP) all-electron basis sets and periodic boundary conditions. This scheme, that has been implemented in the CRYSTAL program for quantum chemistry of the solid state,[15,16] is affected by the somehow general *rigid-atom approximation* that requires an arbitrary partition of the total *static* electron charge density (ECD) $\rho(\mathbf{r})$ of the system into subvolumes associated with each atom that is implicitly retained also when nuclear motions are considered.[17]

Few implementations of *ab initio* atomic DW thermal factors in a plane-wave basis representation (where atomic cores are treated with pseudo-potentials or PAWs,

projected augmented waves) have appeared in the literature that are expressed in terms of "generalized" density of states[18,19] or the cumulant expansion.[20,21] We present here an implementation that is based on an atom-centered orbital basis representation which is expected to be maximally compatible with the atomic partition of the ECD required by the rigid-atom approximation. All-electron basis sets are considered with which core and valence electrons are treated at the same level of accuracy. The effect of the computational parameters involved in such an approach is investigated into details.

A *direct comparison* between computed data and primary experimental data, such as the dynamical structure factors, is also relevant for the assessment of merits and limits of different solid state quantum chemical methods, that are usually discussed with respect to energy or energy-related properties (equilibrium structure, vibrational spectra, thermodynamical properties, etc.). In recent years, for instance, availability of high-resolution Compton profiles (primary observables in momentum space) from synchrotron radiation sources has allowed for a critical discussion of the intrinsic limitations of Kohn-Sham[22] DFT in describing the distribution of electron velocities in crystals.[23–30]

On the other hand, in general, experimental diffraction intensities and charge densities are less accurate than energy-related properties.[31] Crystalline silicon represents an exception because of the high level of purity of its single crystals and availability of a very accurate technique for the measurement of dynamical structure factors (Pendellösung fringes method)[32–35] which are known by an order of magnitude more accurately than for any other crystal.[17]

In this paper we apply the above-mentioned scheme to crystalline silicon. This technique relies on a proper description of both the *lattice dynamics* and the *electron charge density* of the system. When use is made of an approximated Hamiltonian (a common practice in solid state quantum chemistry) the determination of different properties may be affected in different ways: poor vibrational frequencies and good charge density, for instance, or viceversa. In the present scheme the simulation of these two contributions is factorized into separable steps so that different methods can be combined together. One of the aims of this work is to critically discuss the delicate effect of the computational setup of *ab initio* schemes when applied to the simulation of dynamical structure factors.

The structure of the paper is as follows: In Section II we report the fundamental equations of quantum lattice dynamics and derive a simple analytical expression for the atomic anisotropic displacement parameters of crystals within the harmonic approximation; atomic Debye-Waller thermal factors are then defined that are commonly adopted for the inclusion of nuclear motion effects on computed X-ray structure factors. Section III reports the computational parameters used in the simulations to be presented in Section IV as concerns the *ab initio* prediction of dynamical structure factors of crystalline silicon. Conclusions are drawn in Section V.

II. FROM PHONONS TO DEBYE-WALLER FACTORS

In this section we briefly recall some basic equations of standard quantum lattice dynamics used to obtain a simple expression for the atomic anisotropic displacement parameters (ADP) of crystals within the harmonic approximation. The connection between ADPs and Debye-Waller atomic thermal factors that usually account for the nuclear motion when computing X-rays structure factors is then illustrated. Even if the formalism used is well known, we believe that it is worth being recalled here explicitly for two reasons: i) it is expedient to introduce all the parameters in the theory whose effect shall be discussed in the following sections; ii) the rigorous definition of ADPs and related quantities is not unique in the literature (see for instance the IUCr report about this, Ref. 13).

A. Elements of Lattice Dynamics

A three-dimensional crystal can be regarded as a periodic array of atoms interacting with one another; in the presence of interatomic interactions the static (non-vibrating) crystal assumes an equilibrium configuration $\mathcal{R}_0 \equiv \{\dots\ ,\ [(\mathbf{R}_0)_a + \mathbf{g}]\ ,\ \dots\}$ that is unambiguously defined by the equilibrium positions $\{(\mathbf{R}_0)_a\}$ of the N atoms of the cell ($a = 1, \dots, N$); the lattice vector $\mathbf{g} = \sum_{m=1}^{3} l_m^g\, \mathbf{a}_m$ identifies the general crystal cell where $\mathbf{a}_m$ are the direct lattice basis vectors: in a cyclic crystal model (*i.e.* within Born von Kármán periodic boundary conditions) the integers l_m^g run from 0 to $L_m - 1$. In cubic crystals, as in the present case, all L_m's are set to a common value L. Parameter L defines the size of a supercell (SC).When nuclear motion (due to Heisenberg principle, finite temperature or other external perturbations) is considered, the atomic equilibrium positions become the static average positions of the atoms displaced by $\mathbf{x}_a^{\mathbf{g}}$ which define the general configuration $\mathcal{R} \equiv \{\dots\ ,\ [(\mathbf{R}_0)_a + \mathbf{g} + \mathbf{x}_a^{\mathbf{g}}]\ ,\ \dots\}$. In what follows, matrix notation is used extensively; uppercase letters in bold and lowercase letters in bold with over-line represent $3N \times 3N$ matrices and $3N$ vectors, respectively. Thus, the Cartesian coordinates of the displacements are represented by vectors $\overline{\mathbf{x}^{\mathbf{g}}}$. By working within the Born-Oppenheimer approximation, expanding in a Taylor series the lattice potential $V(\mathcal{R})$ (*i.e.* potential energy per cell) with respect to these coordinates about the equilibrium $\mathcal{R}_0$ configuration, after setting $V(\mathcal{R}_0) = 0$, and exploiting translational invariance, the usual expression

is obtained:

$$V(\mathcal{R}) = \frac{L^3}{2} \sum_{\mathbf{g}} \left(\overline{\mathbf{x}}^{\mathbf{0}}\right)^T \mathbf{V}^{\mathbf{g}} \overline{\mathbf{x}}^{\mathbf{g}} + \mathcal{O}_3(\{\overline{\mathbf{x}}^{\mathbf{g}}\}) \,. \qquad (1)$$

In the following we shall extensively use the *harmonic approximation* which neglects all $\mathcal{O}_3$ terms in equation (1) where we have introduced the Hessian matrices $\{\mathbf{V}^{\mathbf{g}}\}$ to be used below whose elements are the second derivatives of the total energy per cell with respect to the atomic displacements.[36]

Each of the L^3 independent equations originated from the harmonic Schrödinger equation for the nuclear motion is associated with a wavevector $\mathbf{k} = \sum_{n=1}^{3} (\kappa_n/L)\, \mathbf{b}_n$ where $\mathbf{b}_n$ are the reciprocal lattice vectors and the integers κ_n run from 0 to $L-1$.[37] For each $\mathbf{k}$, the *dynamical matrix* $\mathbf{W}^{\mathbf{k}}$ is defined as Fourier transform (FT) of the Hessian matrices $\{\mathbf{V}^{\mathbf{g}}\}$:

$$\mathbf{W}^{\mathbf{k}} = \sum_{\mathbf{g}=1}^{L^3} \mathbf{M}^{-\frac{1}{2}} \mathbf{V}^{\mathbf{g}} \mathbf{M}^{-\frac{1}{2}} \, \exp(\imath \mathbf{k} \cdot \mathbf{g}) \,, \qquad (2)$$

where $\mathbf{M}$ is the diagonal matrix of the nuclear masses. The solution is then obtained through diagonalization of the L^3 matrices $\left\{\mathbf{W}^{\mathbf{k}}\right\}$ by the following unitary transformation:

$$(\mathbf{U}^{\mathbf{k}})^{\dagger} \, \mathbf{W}^{\mathbf{k}} \, \mathbf{U}^{\mathbf{k}} \;=\; \mathbf{\Lambda}^{\mathbf{k}} \quad \text{with} \quad (\mathbf{U}^{\mathbf{k}})^{\dagger} \mathbf{U}^{\mathbf{k}} = \mathbf{I} \,. \qquad (3)$$

The eigenvalues are related to the *vibrational frequencies* $\nu_i^{\mathbf{k}} = \sqrt{\lambda_i^{\mathbf{k}}}$ (here and in the following atomic units are adopted), while the columns of the $\mathbf{U}^{\mathbf{k}}$ matrix describe the *normal modes*:

$$\overline{\mathbf{q}}^{\mathbf{k}} = \mathbf{M}^{\frac{1}{2}} (\mathbf{U}^{\mathbf{k}})^{\dagger} \overline{\mathbf{x}}^{\mathbf{k}} \quad \text{with} \quad \overline{\mathbf{x}}^{\mathbf{k}} = \frac{1}{\sqrt{L^3}} \sum_{\mathbf{g}=1}^{L^3} \overline{\mathbf{x}}^{\mathbf{g}} \, \exp(\imath \mathbf{k} \cdot \mathbf{g}) \,.$$

To each $\mathbf{k}$-point in the first Brillouin zone, $3N$ oscillators (*i.e.* phonons) are associated which are labeled by a *phonon band index* i ($i = 1, \ldots, 3N$). It proves useful to introduce at this stage a new set of coordinates (*frequency scaled coordinates*) $\overline{\xi}^{\mathbf{k}} = (\mathbf{\Lambda}^{\mathbf{k}})^{\frac{1}{4}} \overline{\mathbf{q}}^{\mathbf{k}}$ in unity of the classical elongation. The correspondence $\mathcal{R} \longleftrightarrow \{x_i^{\mathbf{g}}\} \longleftrightarrow \{q_i^{\mathbf{k}}\} \longleftrightarrow \{\xi_i^{\mathbf{k}}\}$ is implicit here and in the following.

In principle, equation (2) can be used to compute, and then diagonalize according to equation (3), the dynamical matrices of just the L^3 $\mathbf{k}$-points defined above. However, if long-range electrostatic contributions to the energy second derivatives $\{\mathbf{V}^{\mathbf{g}}\}$ vanish within the portion of the crystal spanned by the sum over direct lattice vectors $\mathbf{g}$ in equation (2), then, from the definition of discrete FT, such an expression can be used to construct the dynamical matrices of a denser set of $\mathbf{k}$-points represented by a parameter $L' \geq L$. Such an *interpolation technique*, to be used in Section IV, can be quite effective in the case of a fully covalent crystal as crystalline silicon without long-range electrostatic contribution to the total energy. On the contrary, when such electrostatic contributions become relevant (as in ionic crystals), they have to be explicitly accounted for with appropriate corrections.[38–40]

The complete harmonic Hamiltonian for the nuclear motion, as a function of the ξ coordinates, is splitted as

$$\hat{H} = \sum_{i,\mathbf{k}} \hat{H}_i^{\mathbf{k}} \quad \text{with} \quad \hat{H}_i^{\mathbf{k}} = \frac{\sqrt{\lambda_i^{\mathbf{k}}}}{2} \left[-\frac{\partial^2}{\partial (\xi_i^{\mathbf{k}})^2} + (\xi_i^{\mathbf{k}})^2 \right] \,.$$

The solutions, in terms of eigenvectors and eigenvalues, of the harmonic oscillator Schrödinger equation, $\hat{H}_i^{\mathbf{k}} \mathbb{H}_{m_i^{\mathbf{k}}} = \varepsilon_{m_i^{\mathbf{k}}} \mathbb{H}_{m_i^{\mathbf{k}}}$, are well known:

$$\varepsilon_{m_i^{\mathbf{k}}} = \left(m_i^{\mathbf{k}} + \frac{1}{2} \right) \frac{\sqrt{\lambda_i^{\mathbf{k}}}}{2\pi} \quad \text{and} \quad \mathbb{H}_{m_i^{\mathbf{k}}} = N_{m_i^{\mathbf{k}}} e^{-\frac{(\xi_i^{\mathbf{k}})^2}{2}} \mathcal{H}_{m_i^{\mathbf{k}}} \,,$$

where $N_{m_i^{\mathbf{k}}}$ is a normalization factor and $\mathcal{H}_{m_i^{\mathbf{k}}}$ is the m-order *Hermite polynomial*. Let us introduce here the following property of the eigenfunctions of the quantum harmonic oscillator that will be used below:

$$\int d\xi_i^{\mathbf{k}} (\xi_i^{\mathbf{k}})^2 \left| \mathbb{H}_{m_i^{\mathbf{k}}} \right|^2 = \frac{2 m_i^{\mathbf{k}} + 1}{2} \,. \qquad (4)$$

The general eigenfunction and the corresponding eigenvalue of $\hat{H}$ are identified by the vector of non-negative integers $M = \{\ldots, m_1^{\mathbf{k}}, \ldots, m_{3N}^{\mathbf{k}}, \ldots\}$, which assigns the level of excitation of all vibrational modes:

$$\Psi_M(\mathcal{R}) = \prod_{i,\mathbf{k}} \mathbb{H}_{m_i^{\mathbf{k}}} \quad \text{and} \quad E_M = \sum_{i,\mathbf{k}} \varepsilon_{m_i^{\mathbf{k}}} \,. \qquad (5)$$

According to standard statistical mechanics, the Boltzmann probability distribution function (PDF) for the nuclei at a temperature T can be expressed as follows:

$$\begin{aligned} \mathrm{P}_T(\mathcal{R}) \;&=\; \frac{1}{Z(T)} \sum_M e^{-\frac{E_M}{k_B T}} \, |\Psi_M(\mathcal{R})|^2 \,; \\ Z(T) \;&=\; \sum_M e^{-\frac{E_M}{k_B T}} \,, \end{aligned} \qquad (6)$$

where k_B is Boltzmann's constant and $Z(T)$ is the *partition function*:

$$Z(T) = \prod_{i,\mathbf{k}} Z_i^{\mathbf{k}}(T) \quad \text{with} \quad Z_i^{\mathbf{k}}(T) = \sum_{m_i^{\mathbf{k}}=0}^{\infty} e^{-\frac{\varepsilon_{m_i^{\mathbf{k}}}}{k_B T}} \,. \qquad (7)$$

Substitution of equation (7) into equation (6) and use of the simple dependence of E_M on the excitation levels, leads to the following compact expression of the probability distribution for the nuclei in the *harmonic* [(h)] *approximation*:

$$\begin{aligned} \mathrm{P}_T^{(\mathrm{h})}(\mathcal{R}) \;&=\; \prod_{i,\mathbf{k}}{}' \, \mathrm{p}_T^{(\mathrm{h})}(\xi_i^{\mathbf{k}}) \quad ; \\ \mathrm{p}_T^{(\mathrm{h})}(\xi_i^{\mathbf{k}}) \;&=\; \left(1 - e^{-\frac{\nu_i^{\mathbf{k}}}{2\pi k_B T}} \right) \sum_{m_i^{\mathbf{k}}=0}^{\infty} e^{-\frac{m_i^{\mathbf{k}} \nu_i^{\mathbf{k}}}{2\pi k_B T}} \left| \mathbb{H}_{m_i^{\mathbf{k}}} \right|^2 \,. \end{aligned} \qquad (8)$$

The product $\prod'$ excludes the three zero-frequency modes which correspond to pure translations. From the above expression, it is seen that the harmonic approximation implies all the PDFs, $\mathrm{p}_T^{(\mathrm{h})}(\xi_i^{\mathbf{k}})$, to be Gaussian functions: $\mathrm{p}_T^{(\mathrm{h})}(\xi_i^{\mathbf{k}}) \equiv \mathrm{G}_T(\xi_i^{\mathbf{k}};\sigma_{i,T}^{\mathbf{k}})$ where the variance is defined in the standard way and then leads to:

$$\begin{aligned}\left(\sigma_{i,T}^{\mathbf{k}}\right)^2 &\equiv \int \mathrm{d}\xi_i^{\mathbf{k}} \left(\xi_i^{\mathbf{k}}\right)^2 \left[\mathrm{p}_T^{(\mathrm{h})}(\xi_i^{\mathbf{k}})\right] = \left(1-e^{-\frac{\nu_i^{\mathbf{k}}}{2\pi k_B T}}\right) \sum_{m_i^{\mathbf{k}}=0}^{\infty} e^{-\frac{m_i^{\mathbf{k}}\nu_i^{\mathbf{k}}}{2\pi k_B T}} \int \mathrm{d}\xi_i^{\mathbf{k}} \left(\xi_i^{\mathbf{k}}\right)^2 \left|\mathbb{H}_{m_i^{\mathbf{k}}}\right|^2 \\ &= \left(1-e^{-\frac{\nu_i^{\mathbf{k}}}{2\pi k_B T}}\right) \sum_{m_i^{\mathbf{k}}=0}^{\infty} \left[\left(m_i^{\mathbf{k}} e^{-\frac{m_i^{\mathbf{k}}\nu_i^{\mathbf{k}}}{2\pi k_B T}}\right) + \frac{1}{2} e^{-\frac{m_i^{\mathbf{k}}\nu_i^{\mathbf{k}}}{2\pi k_B T}}\right] = \left[\frac{1}{e^{\frac{\nu_i^{\mathbf{k}}}{2\pi k_B T}}-1} + \frac{1}{2}\right] . \end{aligned} \tag{9}$$

Here, in the second step we took advantage of property (4) while in the third we considered the convergence of a well-known series.[41] Let us come back to the expression of the harmonic probability distribution for the nuclei in equation (8) and work it out as follows:

$$\begin{aligned}\mathrm{P}_T^{(\mathrm{h})}(\mathcal{R}) &= \prod_{i,\mathbf{k}}{}' \mathrm{G}_T(\xi_i^{\mathbf{k}};\sigma_{i,T}^{\mathbf{k}}) \\ &\propto \prod_{i,\mathbf{k}}{}' \exp\left[-\left(\xi_i^{\mathbf{k}}\right)^2 / 2\left(\sigma_{i,T}^{\mathbf{k}}\right)^2\right] \\ &\propto \exp\left[-1/2 \sum_{\mathbf{k}=1}^{L^3} \left(\overline{\xi}^{\mathbf{k}}\right)^{\dagger} \left(\Xi^{\mathbf{k}}\right)^{-1} \overline{\xi}^{\mathbf{k}}\right] , \end{aligned} \tag{10}$$

where we have introduced the diagonal matrix $\Xi^{\mathbf{k}}$ whose elements are the $3N$ variances of equation (9) for $i = 1,\ldots,3N$. Now, by considering the definition of the frequency scaled coordinate, relationships (4) and focusing on the atoms in the reference cell ($\mathbf{g}=\mathbf{0}$), we obtain:

$$\mathrm{P}_T^{(\mathrm{h})}(\mathcal{R}) \propto \exp\left[-1/2 \left(\overline{\mathbf{x}}^{\mathbf{0}}\right)^T \left(\mathbf{X}^{\mathbf{0}}\right)^{-1} \overline{\mathbf{x}}^{\mathbf{0}}\right] , \tag{11}$$

where the $\mathbf{X}^{\mathbf{0}}$ matrix is expressed as

$$\mathbf{X}^{\mathbf{0}} = \frac{1}{L^3} \sum_{\mathbf{k}=1}^{L^3} \mathbf{M}^{-\frac{1}{2}} \mathbf{U}^{\mathbf{k}} (\mathbf{\Lambda}^{\mathbf{k}})^{-\frac{1}{4}} \Xi^{\mathbf{k}} (\mathbf{\Lambda}^{\mathbf{k}})^{-\frac{1}{4}} \left(\mathbf{U}^{\mathbf{k}}\right)^{\dagger} \mathbf{M}^{-\frac{1}{2}} .$$

As will be discussed in the next section, the above matrix turns out to be the mean squared displacement tensor whose diagonal 3×3 blocks define the so-called anisotropic atomic displacement tensors.

B. Atomic Anisotropic Displacement Parameters

In the previous section we anticipated that the $\mathbf{X}^{\mathbf{0}}$ matrix can be interpreted as the mean squared displacement tensor. This can be seen on the grounds of the classical approach to quadratic forms: when a Gaussian probability density function is considered in the form of equation (11), then, $\mathbf{X}^{\mathbf{0}}$ is the *second-moment* or *covariance* matrix with elements $\langle x_i^{\mathbf{0}} x_j^{\mathbf{0}} \rangle_T^{(\mathrm{h})}$, where $\langle\cdots\rangle^{(\mathrm{h})}$ denotes the expectation with respect to the Gaussian (harmonic) probability density of the displacements at a temperature T. Even if the harmonic approximation is known to provide an accurate description of many crystals, its deficiencies are well-known: for instance, a crystal with harmonic interatomic forces does not undergo any lattice thermal expansion.[12] Usually, only the N 3×3 diagonal blocks $\mathbf{X}_a^{\mathbf{0}}$ of $\mathbf{X}^{\mathbf{0}}$ are considered that are the atomic anisotropic displacement tensors which are used, in different forms, in the expression of the atomic Debye-Waller factors for the description of dynamical X-rays structure factors (as described in the next section); off-diagonal blocks bring information about the coupling of the motions of different atoms. It has recently been shown that diagonal ADPs already provide a good description of the thermal nuclear motion of a delicate class of materials as molecular crystals.[42]

If $\mathbf{X}_a^{\mathbf{0}}$ is positive definite then the surfaces of constant probability defined by equation

$$\left(\mathbf{x}_a^{\mathbf{0}}\right)^T \left(\mathbf{X}_a^{\mathbf{0}}\right)^{-1} \mathbf{x}_a^{\mathbf{0}} = \text{constant} , \tag{12}$$

are *ellipsoids* enclosing some finite probability for atomic displacement.[9] The length of the principal semi-axes of the ellipsoid and their orientation are given by the eigenvalues and eigenvectors of $\mathbf{X}_a^{\mathbf{0}}$, respectively. The eigenvalues, usually expressed in units of 10^{-4} Å, are commonly referred to as *atomic displacement parameters* (ADP). The symmetry of crystalline silicon imposes the $\mathbf{X}_{Si}^{\mathbf{0}}$ tensors to be diagonal and isotropic. In this case, the commonly considered Debye-Waller parameter B is simply: $B = 8\pi^2 \times$ ADP.

C. Static and Dynamical Structure Factors

In determination of the X-ray structure factors, the *rigid-atom approximation* is commonly adopted which

implies a linear partitioning of the continuous static electron charge density (ECD) $\rho_{\rm cell}(\mathbf{r})$ into subvolumes associated with scattering centers that usually coincide with the N atoms per cell:[17] $\rho_{\rm cell}(\mathbf{r}) = \sum_a \rho_a(\mathbf{r}-(\mathbf{R}_0)_a)$. Note that this partitioning is rather arbitrary: real space[43,44] as well as basis set[45] partitioning can be adopted; in this study a Mulliken partition is used. We can associate with each atom an *atomic scattering factor* $f_a(\mathbf{p})$ defined as the FT of the corresponding atomic electron density $\rho_a(\mathbf{r})$ (we consider the atom in the origin). A strong approximation comes into the picture when we consider the dynamics of the atoms as it is assumed that the electronic density $\rho_a(\mathbf{r})$ follows the motion of the atom rigidly and instantaneously. We introduce the probability $p_a(\mathbf{r})$ of finding atom a at position $\mathbf{r}$ and the static electronic density at $\mathbf{r}$ when the atomic center is at $\mathbf{r}'$: $\rho_a(\mathbf{r}-\mathbf{r}')$. Now we can write the atomic dynamical electronic density as the following convolution:

$$\tilde{\rho}_a(\mathbf{r}) = \int \mathrm{d}\mathbf{r}' \rho_a(\mathbf{r}-\mathbf{r}') p_a(\mathbf{r}') \equiv \rho_a(\mathbf{r}) * p_a(\mathbf{r}) \ . \quad (13)$$

The dynamic atomic scattering factor $\tilde{f}_a(\mathbf{p})$ can be calculated from Fourier transforming equation (13):

$$\tilde{f}_a(\mathbf{p}) = f_a(\mathbf{p}) \times q_a(\mathbf{p}) \ , \quad (14)$$

where $q_a(\mathbf{p})$ is the FT of $p_a(\mathbf{r})$. This term is also known as the Debye-Waller (DW) atomic thermal factor. As shown above, if we consider the harmonic lattice potential then the atomic probability density function $p_a(\mathbf{r})$ has the form of a Gaussian function:

$$p_a(\mathbf{r}) = (2\pi)^{-\frac{3}{2}} \times (\det \mathbf{X}_a)^{-\frac{1}{2}} \times e^{-\frac{1}{2}\mathbf{r}^T \mathbf{X}_a^{-1} \mathbf{r}} \ , \quad (15)$$

and the corresponding DW factor takes the form:

$$q_a(\mathbf{p}) = e^{-\frac{1}{2}\mathbf{p}^T \mathbf{X}_a \mathbf{p}} \ . \quad (16)$$

The scattering factor $\tilde{F}_\infty(\mathbf{p})$ of the whole crystal (*i.e.* the amplitude of the scattered wave) can be expressed as:

$$\begin{aligned} \tilde{F}_\infty(\mathbf{p}) &= \sum_{a \in \text{cell}} f_a(\mathbf{p}) \sum_{\mathbf{K}} q_a(\mathbf{p}) e^{i\mathbf{p}\cdot(\mathbf{R}_0)_a} \delta(\mathbf{K}-\mathbf{p}) \\ &= \begin{cases} 0 & \text{if} \quad \mathbf{p} \neq \mathbf{K} \\ \\ \tilde{F}_{hkl} & \text{if} \quad \mathbf{p} = \mathbf{K} \ \text{ Bragg's condition} \ , \end{cases} \end{aligned} \quad (17)$$

where $\mathbf{K} = h\mathbf{b}_1 + k\mathbf{b}_2 + l\mathbf{b}_3$ is a reciprocal lattice vector (hkl are Miller's indexes) and the dynamical structure factors $\{\tilde{F}_{hkl}\}$ of a crystal within harmonic approximation are then defined as

$$\tilde{F}_{hkl} = \sum_{a \in \text{cell}} f_a(\mathbf{K}) \times e^{i2\pi\mathbf{K}\cdot(\mathbf{R}_0)_a} \times \underbrace{e^{-\frac{1}{2}\mathbf{K}^T \mathbf{X}_a^{\mathbf{0}} \mathbf{K}}}_{\text{DW factor}} \quad (18)$$

III. COMPUTATIONAL DETAILS

All calculations were performed using the "periodic" *ab initio* CRYSTAL program.[15,16] All quantities of interest in the program are expressed in terms of atomic orbitals, AO, wave-functions, each one being a linear combination of Gaussian "primitive" functions centered in high-symmetry positions: these AOs constitute the so-called basis set (BS). As concerns the structure, within the harmonic approximation, here extensively used, no lattice expansion can be predicted so that the experimental equilibrium lattice parameter at 298 K ($\mathbf{a} = 5.4307$ Å) was used. In principle, however, linear thermal expansion coefficients could be computed within the so-called quasi-harmonic approximation[46,47] by minimizing Helmholtz's free energy (computed from the whole phonon dispersion of the crystal) at a given temperature, as a function of the cell volume or, alternatively, from the knowledge of the isothermal bulk modulus, the mode Grüneisen parameters and the mode contributions to the specific heat.[48]

Four one-electron Hamiltonians are considered: the classical HF, two typical DFT (a local LDA[49] and the generalized-gradient PBE[50]) and a hybrid (B3LYP)[51] one. The accurate calibration of the basis set is perhaps the most delicate step in defining the optimal computational setup and is discussed in details below.In CRYSTAL, the truncation of infinite lattice sums is controlled by five thresholds, which are here set to 8,8,8,8,16. The DFT exchange-correlation contribution is evaluated by numerical integration over the cell volume: radial and angular points of the atomic grid are generated through Gauss-Legendre and Lebedev quadrature schemes, using a (75,974) pruned grid. Reciprocal space is sampled in a regular sublattice with a shrinking factor equal to 8 corresponding to 29 $\mathbf{k}$-points in the irreducible Brillouin zone.

In a recent study concerning the *ab initio* simulation of the density matrix of crystalline solids,[52] we have analyzed the performance of different AO-BSs in the computation of two quantities related to the ECD of silicon: the value of $\rho(\mathbf{r})$ at the bond midpoint, and the F_{222} structure factor (whose non-zero value is a measure of the asphericity of the ECD about the individual atoms). For comparison, calculations were performed with the Quantum-ESPRESSO code,[53] where a plane-wave (PW) BS was used for the valence electrons, while the core contribution was described with the PAW (Projector Augmented Waves) technique. In both cases the PBE Hamiltonian was adopted. A clear convergence of AO-BSs to PW-BS was reported.

In the present work, we adopt the 6-21G* split-valence plus polarization basis set used in that work and explicitly reported in Ref. 54, to be indicated as BS1 in the following. A second much reacher BS is considered, that is BS1 enriched by three sets of single-primitive *polarization* functions, one of d and two of f type with exponents of 0.3, 0.8, 0.2 a.u., respectively: this BS will be referred to as BS2.

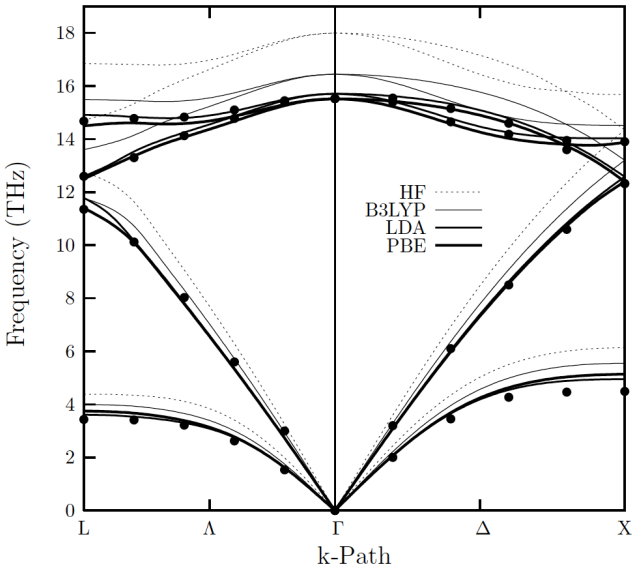

FIG. 1: Phonon dispersion branches of crystalline silicon along two high-symmetry path within the first Brillouin zone (Γ - X and Γ - L) as computed with four different Hamiltonians with the BS1 basis set and compared to experimental data (black dots) from Ref. 55.

IV. RESULTS AND DISCUSSION

The technique that we are discussing for the *ab initio* simulation of dynamical X-ray structure factors relies on a correct description of two aspects of crystalline materials: lattice vibrations and electron charge density which correspond to two distinct steps in our scheme. These properties are computationally related to different quantities, energy derivatives and density matrix, respectively, so that different computational approaches can behave differently on these respects. The following two subsections are devoted to the discussion of the effects of the adopted Hamiltonian and basis set on lattice dynamics and static charge density of crystalline silicon in order to define an optimal computational setup.

A. Vibrational frequencies and ADPs

The accuracy of a given method in describing lattice dynamics is usually checked in terms of vibration frequencies (eigenvalues $\mathbf{\Lambda^k}$ of the dynamical matrices in equation 3) in the form of dispersion branches (like those reported in Figure 1) which are accessible to neutron inelastic scattering experiments[55] or of thermodynamical properties, such as the entropy or the Gibbs free energy, which in turn depend on the vibration frequencies alone. Such a validation, however, is not completely satisfactory in this case because in our scheme we consider not only the eigenvalues but also the eigenvectors $\mathbf{U^k}$ (equation 3) which are used to construct ADPs in equation (12).

TABLE I: ADP (in 10^{-4} Å^2) of crystalline silicon as computed at $T = 298.15$ K with the BS1 and BS2 basis sets on a conventional supercell as a function of the adopted Hamiltonian with (first column) $L \equiv L' = 2$ and (second column) $L = 2$ and $L' = 48$ where $L = 2$ corresponds to 32 **k**-points and $L' = 48$ to 442368 **k**-points where the dynamical matrices of equations (2 - 3) are diagonalized (see the description of the Hessian interpolation technique in Section II A). For the PBE functional, results are also shown for intermediate basis sets to highlight convergence.

	$\hat{H}$	$L \rightarrow L'$	
		2→2	2→48
BS1	HF	34.09	40.89
	B3LYP	40.35	48.75
	PBE	45.97	55.41
	LDA	46.69	56.20
BS1+*d*	PBE	49.48	58.17
BS1+*df*	PBE	51.73	60.96
BS2	HF	35.46	42.74
	B3LYP	41.21	49.43
	PBE	51.95	61.11
	LDA	56.64	67.87

The effect of the Hamiltonian is shown in Figure 1 and Table I as concerns vibrational frequencies and normal modes, respectively. Figure 1 reports dispersion branches of crystalline silicon along two high-symmetry paths within the first Brillouin zone (Γ - X and Γ - L) as computed with four different Hamiltonians (representatives of different classes of one-electron methods: HF, B3LYP, PBE and LDA) with the BS1 basis set at the experimental geometry. The effect of the Hamiltonian is dramatic: they all describe the shape of the branches reasonably well but they are blue-shifted in the energy axis with respect to the experiment in the order HF > B3LYP > PBE ≈ LDA. The large blue-shift in HF and B3LYP is probably due to the fact that these methods describe very rigid covalent bonds (see, for instance, the ECD at the bond midpoint in Section IV B). The PBE functional of the DFT is found to provide the best agreement with the experimental frequencies of Ref. 55 (black points in the figure).

In Figure 1 we do not report the effect of BS on the computed vibrational frequencies explicitly for reasons of clarity. BS2 results in relatively small variations with respect to BS1, as compared to different Hamiltonians. For instance, the optical frequency at Γ, computed with the PBE functional, passes from 15.52 to 15.53 THz which would not be visible on that scale.

TABLE II: ADP of crystalline silicon (in 10^{-4} Å^2) as computed at $T = 298.15$ K with the PBE functional of the DFT and the BS2 basis set as a function of the adopted supercell (SC). The supercell used is a conventional one (4 times larger than the primitive); the size of the SC is defined by the parameter L while the number of **k**-points used for the Hessian interpolation is related to L' (see text in Section II A). Here $L' = 48$, corresponding to 442368 **k**-points where the dynamical matrices of equations (2 - 3) are diagonalized. The number N of atoms in the SC is also reported.

L	N	$L \rightarrow L$	$L \rightarrow L'$
1	8	45.35	101.91
2	64	51.95	61.11
3	216	54.78	60.71
4	512	57.13	60.55
EXP. (Ref. 56)		59.41 ± 0.21	

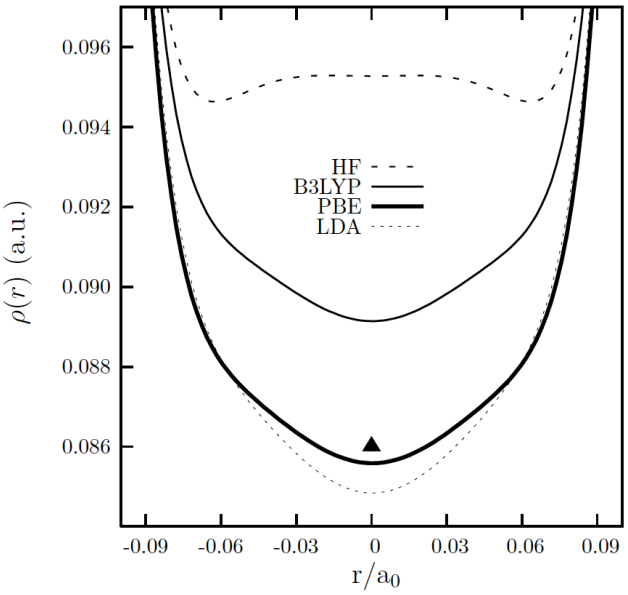

FIG. 2: Electron charge density profile along a Si-Si bond, in the vicinity of its midpoint, in crystalline silicon as computed with different Hamiltonians with the BS2 basis set. The triangle represents the "experimental" value of the static charge density at the midpoint of the bond from Ref. 17.

In Table I we report the computed ADP as obtained with the above-mentioned Hamiltonians and with the two basis sets at $T = 298.15$ K. The following remarks can be inferred from that table:

(i) a strong dependence on the Hamiltonian is observed also for ADP which follows the order HF < B3LYP < PBE < LDA that is opposite to the order in the vibrational frequencies. The ADP is a measure of the mean squared displacement of every silicon atom from its equilibrium position; the more rigid the covalent bonds, the higher the vibration frequencies and the smaller the ADP;

(ii) effects due to the basis set (from BS1 to BS2) are apparent and more pronounced for the pure DFT Hamiltonians (PBE and LDA) with respect to HF and B3LYP because they describe a more diffuse electron distribution. From the data of the table, one could wonder whether BS2 represents or not a converged basis set as concerns the ADPs. Having this purpose in mind, PBE data are also reported for two intermediate basis sets (BS1+*d* and BS1+*df*) which are obtained by progressively adding the polarization functions of BS2 to BS1. BS2 results vary by only 0.2 % with respect to BS1+*df*;

(iii) at variance with vibration frequencies, the ADPs are not direct observables; however, they can be extracted from experimental data by fitting to some theoretical model. The most accurate determination of the ADP of crystalline silicon is 59.41 ± 0.21 10^{-4} Å^2 as obtained by fitting phonon dispersion curves from inelastic neutron data to a harmonic model.[56] Several other "experimental" determinations are available in the literature as derived from X-ray diffraction experiments and they all lie in the range $57 \leq$ ADP ≤ 59 (values in 10^{-4} Å^2).[35,57–60] Thus, the PBE functional is again found to provide the best agreement with experiment when our best BS2 basis set is used;

(iv) the last column in Table I reports the ADP as obtained with a Hessian interpolation (discussed in Section II A) from $L = 2$ to $L' = 48$, that is, from 32 to 442368 **k**-points where the dynamical matrices of equations (2 - 3) are diagonalized. It is seen that the effect of interpolation amounts to 20 %.

We have seen that the PBE functional of the DFT provides the best agreement as concerns both vibrational frequencies and ADP values. We consider, now, the PBE method and we discuss the effect of the "supercell" (SC)size (L)used in the sampling of reciprocal space (number of **k**-points where the dynamical matrix is diagonalized). Table II reports the ADP of silicon as computed with different SCs and with the BS2 basis sets. Interpolations up to $L' = 48$ (442368 **k**-points) are also reported for each SC. The conventional SC with $L = 2$ is the smallest one (only 64 atoms) which already provides a good description of the ADP (61.11 10^{-4} Å^2) while the simple conventional SC with $L = 1$ is clearly insufficient.

We can see how the effect of the Hessian interpolation described in Section II A is reduced while increasing the size L of the starting SC: it goes from 55 % of ADP

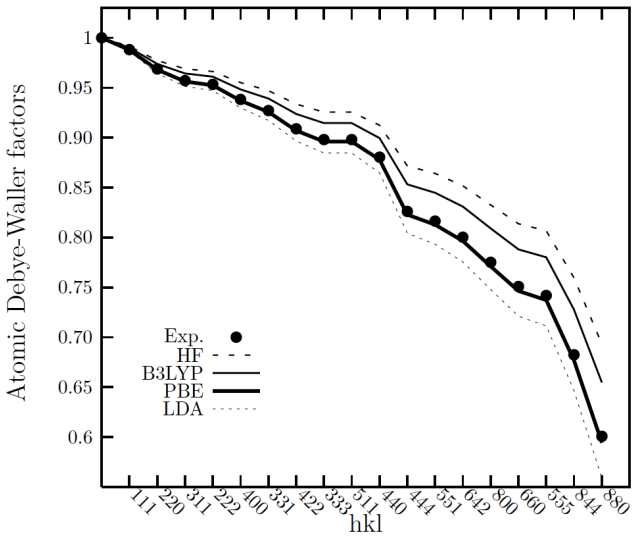

FIG. 3: Atomic Debye-Waller damping factors at 298 K, as defined in equation (18), computed with four different Hamiltonians from their respective best determinations of the ADP for the set of 18 structure factors of Ref. 17 for silicon. The experimental points correspond to the ADP of Ref. 56.

for $L = 1$ to just 5 % for $L = 4$. Interpolation from a conventional SC with $L = 4$ (512 atoms) gives 60.55 10^{-4} Å^2, which is our best theoretical determination of the ADP, to be compared with the "experimental" value of 59.41 ± 0.21 10^{-4} Å^2 of Ref. 56.

B. Electron charge density

The second step of the technique involves the *ab initio* description of the static charge density $\rho(\mathbf{r})$ of the system.

Both BS1 and BS2 basis sets correctly describe the static ECD of crystalline silicon, BS2 being slightly better. In order to quantify it, we consider the consolidated set of 18 static structure factors by Lu *et al.*[17] and we introduce the so-called agreement factor:

$$R^X = \frac{1}{18} \sum_{hkl} \frac{|F^X_{hkl} - F^{exp}_{hkl}|}{F^{exp}_{hkl}} \times 100 \qquad (19)$$

where X represents the computational method. With the PBE functional, we get $R^{BS1} = 0.15$ % and $R^{BS2} = 0.14$ %.

Again, the effect of the Hamiltonian is dramatic. In Figure 2 we report the computed ECD of crystalline silicon along a Si-Si bond, in the vicinity of its midpoint, as computed with the four Hamiltonians with BS2 basis set. We also report an "experimental" value of the static charge density at the midpoint of the bond from Ref. 17 (black triangle). As expected, DFT provides a very good description of the ECD of the system, PBE being better than LDA. The HF method describes too rigid covalent bonds (see also the discussion in Section IV A) with a very high charge density in the bond region; the hybrid B3LYP schemes obviously lies in between.

TABLE III: Dynamical structure factors $\tilde{F}_{hkl}$ as computed with four different Hamiltonians with the BS2 basis set and with the best determination of the ADP for each Hamiltonian. Experimental values are form Ref. 61. In the last row, overall agreement factors, as defined in equation (19) are reported with respect to the experiment.

hkl	LDA	HF	B3LYP	PBE	EXP.
111	10.590	10.648	10.642	10.601	10.603
220	8.351	8.420	8.410	8.374	8.388
311	7.638	7.718	7.704	7.669	7.681
400	6.943	7.080	7.039	6.986	6.996
331	6.652	6.838	6.773	6.702	6.726
422	6.037	6.230	6.169	6.093	6.112
333	5.700	5.896	5.838	5.759	5.781
511	5.717	5.919	5.858	5.775	5.791
440	5.250	5.470	5.402	5.313	5.332
444	4.028	4.272	4.202	4.100	4.124
551	3.841	4.088	4.017	3.914	3.935
642	3.557	3.807	3.736	3.631	3.656
800	3.155	3.408	3.336	3.229	3.249
660	2.818	3.072	3.000	2.892	2.914
555	2.703	2.956	2.885	2.777	2.801
844	2.063	2.312	2.242	2.134	2.151
880	1.449	1.685	1.617	1.515	1.533
R	2.06 %	3.40 %	1.83 %	0.47 %	

C. Dynamical structure factors from ADPs

The scheme presented here for the computation of dynamical structure factors relies on the accurate determination of the ADPs of equation (12) from which the Debye-Waller atomic factors of equation (18) are computed which damp the static structure factors. In Figure 3 we report the DW damping factors computed with four different Hamiltonians from their respective best determinations of the ADPs for the set of 18 structure factors F_{hkl} of Ref. 17. The experimental points correspond to the ADP of Ref. 56. It is seen that the HF and B3LYP underestimation of the ADP leads to a too small damping, the LDA overestimation leads to an exceedingly large damping while PBE is in very good agreement with experiment.

Finally, we can compare the *ab initio* computed val-

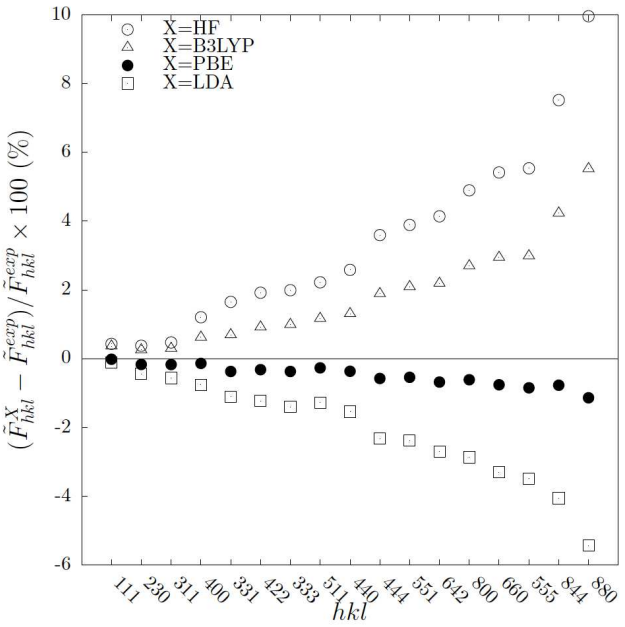

FIG. 4: Percentage differences of dynamical structure factors $\tilde{F}_{hkl}$ of silicon at 298 K as computed with four different Hamiltonians with the BS2 basis set for both the ADPs and the ECD.

ues of dynamical structure factors to their experimental counterparts (see Table III where we report the computed values and compare them to experiment). Let us introduce the index $R^X_{hkl} = (\tilde{F}^X_{hkl} - \tilde{F}^{exp}_{hkl})/\tilde{F}^{exp}_{hkl} \times 100$ which measures the percentage difference of each structure factor $\tilde{F}^X_{hkl}$, computed with method X, with respect to the experimental value.[61] In Figure 4 we report such data for 17 structure factors (the anomalous 222 reflection is omitted) as computed with four different Hamiltonians with the BS2 basis set for both the ADPs and the ECD that is, with the best computational setup for each Hamiltonian. As a general remark, it is seen that the percentage deviations increase at increasing Miller's indices, as expected. HF and B3LYP tend to overestimate the experimental dynamical structure factors by 3.40 % and 1.83 %, respectively; LDA underestimates the experimental data by 2.06 % while PBE, that is the best Hamiltonian for both lattice dynamics and ECD, gives an overall agreement of 0.47 % (on the underestimation side). If we bear in mind that such an agreement is obtained completely *ab initio*, without any fitting to experimental data, the predicting power of this technique can be considered fairly impressive. This excellent agreement, however, might be due to the high symmetry of cubic crystalline silicon; a less satisfactory agreement is expected for low-symmetry multi-atomic crystals.

V. CONCLUSIONS

A fully *ab initio* technique (in the frame of one-electron Hamiltonians and periodic boundary conditions) is here formally presented and discussed for the theoretical description of the effect of temperature on X-ray dynamical structure factors of crystalline materials, which relies on the computation of the atomic anisotropic displacement parameters (ADP) and the Debye-Waller atomic factors within the harmonic approximation. The technique is applied to the simulation of dynamical structure factors of crystalline silicon for which very accurate experimental determinations exist because of the high level of purity of its single crystals and availability of a very accurate technique for measuring the dynamical structure factors (Pendellösung fringes method).

Possibility of including effects of temperature, in a rigorous *ab initio* fashion, in the computed structure factors is appealing since it would reduce the data processing on the experimental side and allow for a direct comparison with the outcomes of X-ray diffraction experiments.

The technique used relies on the accurate description of the lattice dynamics and of the electron charge distribution of the system. The description of both aspects is dramatically affected by the adopted quantum chemical method. In the present case (crystalline silicon), we find that the PBE functional of the DFT provides the best values for both properties.

An overall agreement factor of 0.47 % between the *ab initio* predicted values and the experimental determinations is found, in the best case. This extremely good agreement is probably due to the fact that a simple model based on ADPs is fairly accurate for a simple cubic crystal like silicon. We expect that for multi-atomic low-symmetry compounds, where the somehow arbitrary *rigid atom approximation* severely comes into play, such a simple scheme would prove to be less satisfactory.

Acknowledgments

We acknowledge the CINECA Award N. HP10AX8A2M, 2011 for the availability of high performance computing resources and support.

[1] Dovesi, R.; Civalleri, B.; Roetti, C.; Saunders, V. R. and Orlando, R., *Rev. Comp. Chem.*, 2005, **21**, 1.
[2] Grimme, S.; Antony, J.; Ehrlich, S. and Krieg, H., *J. Chem. Phys.*, 2010, **132**, 154104.
[3] Pisani, C., *Quantum-Mechanical Ab-initio Calculation of the Properties of Crystalline Materials*, Vol. 67 of *Lecture Notes in Chemistry Series*, Springer Verlag, Berlin, 1996.
[4] Dronskowski, R., *Computational Chemistry of Solid State Materials*, Wiley, Weinheim, 2005.
[5] Car, R. and Parrinello, M., *Phys. Rev. Lett.*, 1985, **55**,

2471.

[6] Buda, F.; Car, R. and Parrinello, M., *Phys. Rev. B*, 1990, **41**, 1680.

[7] Vila, F. D.; Lindahl, V. E. and Rehr, J. J., *Phys. Rev. B*, 2012, **85**, 024303.

[8] Pisani, C.; Erba, A.; Ferrabone, M. and Dovesi, R., *J. Chem. Phys.*, 2012, **137**, 044114.

[9] Dunitz, J. D.; Schomaker, V. and Trueblood, K. N., *J. Phys. Chem.*, 1988, **92**, 856.

[10] Dawson, B., *Acta Cryst. A*, 1969, **25**, 12.

[11] Mair, S. L. and Wilkins, S. W., *J. Phys. C: Solid State Phys.*, 1976, **9**, 1145.

[12] Willis, B. T. M., *Acta Cryst. A*, 1969, **25**, 277.

[13] Trueblood, K. N.; Bürgi, H.-B.; Burzlaff, H.; Dunitz, J. D.; Gramaccioli, C. M.; Shulz, H. H.; Shmueli, U. and Abrahams, C., *Acta Cryst. A*, 1996, **52**, 770.

[14] Safarik, D. J.; Llobet, A. and Lashley, J. C., *Phys. Rev. B*, 2012, **85**, 174105.

[15] `CRYSTAL09` user's manual. Dovesi, R.; Saunders, V. R.; Roetti, C.; Orlando, R.; Zicovich-Wilson, C. M.; Pascale, F.; Doll, K.; Harrison, N. M.; Civalleri, B.; Bush, I. J.; D'Arco, P. and Llunell, M.; Università di Torino, Torino, 2010.

[16] Dovesi, R.; Orlando, R.; Civalleri, B.; Roetti, C.; Saunders, V. R. and Zicovich-Wilson, C. M., *Z. Kristallogr.*, 2005, **220**, 571.

[17] Lu, Z. W.; Zunger, A. and Deutsch, M., *Phys. Rev. B*, 1993, **47**, 9385.

[18] Rignanese, G.-M.; Michenaud, J.-P. and Gonze, X., *Phys. Rev. B*, 1996, **53**, 4488.

[19] Lee, C. and Gonze, X., *Phys. Rev. B*, 1995, **51**, 8610.

[20] Vila, F. D.; Rehr, J. J.; Rossner, H. H. and Krappe, H. J., *Phys. Rev. B*, 2007, **76**, 014301.

[21] Rehr, J. J.; Kas, J. J.; Vila, F. D.; Prange, M. P. and Jorissen, K., *Phys. Chem. Chem. Phys.*, 2010, **12**, 5503.

[22] Kohn, W. and Sham, L., *Phys. Rev.*, 1965, **140**, A1133.

[23] Thakkar, A. J. In *Theory and Applications of Computational Chemistry: The First 40 Years*, Dykstra, C. E.; Frenking, G.; Kim, K. S. and Scuseria, G. E., Eds.; Elsevier, Amsterdam, 2005; page 11.

[24] Zope, R. R., *Phys. Rev. A*, 2000, **62**, 064501.

[25] Ragot, S., *J. Chem. Phys.*, 2006, **125**, 014106.

[26] Erba, A.; Pisani, C.; Casassa, S.; Maschio, L.; Schütz, M. and Usvyat, D., *Phys. Rev. B*, 2010, **81**, 165108.

[27] Pisani, C.; Itou, M.; Sakurai, Y.; Yamaki, R.; Ito, M.; Erba, A. and Maschio, L., *Phys. Chem. Chem. Phys.*, 2011, **13**, 933.

[28] Erba, A.; Itou, M.; Sakurai, Y.; Yamaki, R.; Ito, M.; Casassa, S.; Maschio, L.; Terentjevs, A. and Pisani, C., *Phys. Rev. B*, 2011, **83**, 125208.

[29] Pisani, C.; Erba, A.; Casassa, S.; Itou, M. and Sakurai, Y., *Phys. Rev. B*, 2011, **84**, 245102.

[30] Erba, A. and Pisani, C., *J. Comput. Chem.*, 2012, **33**, 822.

[31] Zuo, J. M.; Blaha, P. and Schwarz, K., *J. Phys.: Condens. Matter*, 1997, **9**, 7541.

[32] Saka, T. and Kato, N., *Acta Cryst. A*, 1986, **42**, 469.

[33] Teworte, R. and Bonse, U., *Phys. Rev. B*, 1984, **29**, 2102.

[34] Aldred, P. J. E. and Hart, M., *Proc. R. Soc. London*, 1973, **332**, 223.

[35] Aldred, P. J. E. and Hart, M., *Proc. R. Soc. London*, 1973, **332**, 239.

[36] The elements of these Hessian matrices are defined as $(\mathbf{V^g})_{ai,bj} = \partial^2 V/(\partial x^{\mathbf{0}}_{ai} \partial x^{\mathbf{g}}_{bj})$ and are energy second derivatives with respect to the displacement of atom a along the i-th Cartesian direction in the reference **0** cell and atom b along the j-th Cartesian direction in the **g** crystal cell, with $i,j = x,y,z$. The symmetry of these objects is as follows: $(\mathbf{V^g})_{ai,bj} = (\mathbf{V^{-g}})_{bj,ai}$.

[37] Wallace, D. C., *Thermodynamics of Crystals*, Wiley, New York, USA, 1972.

[38] Wang, Y.; Wang, J.; Wang, Y.; Mei, Z. G.; Shang, S. L.; Chen, L. Q. and Liu, Z. K., *J. Phys.: Condens. Matter*, 2010, **22**, 202201.

[39] Gonze, X. and Lee, C., *Phys. Rev. B*, 1997, **55**, 10355.

[40] Baroni, S.; de Gironcoli, S.; Corso, A. D. and Giannozzi, P., *Rev. Mod. Phys.*, 2001, **73**, 515.

[41] $S(a) = \sum_{n=0}^{\infty} n a^n = \frac{a}{(1-a)^2}$

[42] Madsen, A. Ø.; Civalleri, B.; Ferrabone, M.; Pascale, F. and Erba, A., *Acta Crystallogr. Sec. A*.

[43] Hirshfeld, F. I., *Theor. Chem. Acc.*, 1977, **44**, 129.

[44] Bader, R. F. W., *Atoms in Molecules - A Quantum Theory*, Oxford University Press, Oxford, UK, 1990.

[45] Mulliken, R. S., *J. Chem. Phys.*, 1955, **23**, 1841.

[46] Boyer, L. L., *Phys. Rev. Lett.*, 1979, **42**, 584.

[47] Wei, S.; Li, C. and Chou, M. Y., *Phys. Rev. B*, 1994, **50**, 14587.

[48] Ashcroft, N. W. and Mermin, N. D., *Solid State Physics*, Saunders College, Philadelphia, USA, 1976.

[49] Perdew, J. P. and Zunger, A., *Phys. Rev. B*, 1981, **23**, 5048.

[50] Perdew, J. P.; Burke, K. and Ernzerhof, M., *Phys. Rev. Lett.*, 1996, **77**, 3865.

[51] Becke, A. D., *J. Chem. Phys.*, 1993, **98**, 5648.

[52] Pisani, C.; Dovesi, R.; Erba, A. and Giannozzi, P. In *Modern Charge Density Analysis*, Gatti, C. and Macchi, P., Eds.; Springer, Berlin, 2011.

[53] Giannozzi, P.; Baroni, S.; Bonini, N.; Calandra, M.; R.Car, ; Cavazzoni, C.; Ceresoli, D.; Chiarotti, G. L.; Cococcioni, M.; Dabo, I.; Corso, A. D.; Fabris, S.; Fratesi, G.; de Gironcoli, S.; Gebauer, R.; Gerstmann, U.; Gougoussis, C.; Kokalj, A.; Lazzeri, M.; Martin-Samos, L.; Marzari, N.; Mauri, F.; Mazzarello, R.; Paolini, S.; Pasquarello, A.; Paulatto, L.; Sbraccia, C.; Scandolo, S.; Sclauzero, G.; Seitsonen, A. P.; Smogunov, A.; Umari, P. and Wentzcovitch, R., *J. Phys.: Condens. Matter*, 2009, **21**, 395502.

[54] Pisani, C.; Dovesi, R. and Orlando, R., *Int. J. Quantum Chem.*, 1992, **42**, 5.

[55] Kulda, J.; Strauch, D.; Pavone, P. and Ishii, Y., *Phys. Rev. B*, 1994, **50**, 13347.

[56] Flensburg, C. and Stewart, R. F., *Phys. Rev. B*, 1999, **60**, 284.

[57] Graf, H. A.; Schneider, J. R.; Freund, A. K. and Lehmann, M. S., *Acta Cryst. A*, 1981, **37**, 863.

[58] Fehlmann, M., *J. Phys. Soc. Jpn.*, 1979, **47**, 225.

[59] Krec, K. and Steiner, V., *Acta Cryst. A*, 1984, **40**, 459.

[60] Spackman, M. A., *Acta Cryst. A*, 1986, **42**, 271.

[61] Cummings, S. and Hart, M., *Aust. J. Phys.*, 1988, **41**, 423.